

Rubidium-based multilayer mirrors for soft X-ray radiation

© M.A. Yamshchikova,^{1,2} V.G. Rogachev,¹ A.P. Shkurnov²

¹ Laser Physics Research Institute, Russian Federal Nuclear Center, All-Russian Research Institute of Experimental Physics, 607190 Sarov, Nizhny Novgorod Region, Russia

² Moscow State University, Department of Physics and branch in 607328 Sarov, Nizhny Novgorod Region, Russia
e-mail: ya_maria94@mail.ru

Received July 25, 2024

Revised May 15, 2025

Accepted July 8, 2025

Theoretical study was performed to investigate the configuration of rubidium-based X-ray multilayer mirrors for a wavelength range of 11–17 nm. A genetic algorithm was used to solve the problem of multilayer configuration improvement for such mirrors. A possibility of reaching a maximum theoretical reflectivity limit of 78% for Ru/Rb-mirrors at 13.5 nm and of 83% for Al/Rb-mirrors near 17.0–17.1 nm is justified.

Keywords: X-ray radiation, multilayer metal mirrors, refractive index, reflectivity, spectral selectivity, genetic algorithm.

DOI: 10.61011/TP.2025.10.62094.244-24

Introduction

Development of modern soft X-ray control technologies directly depends on the improvement of optical properties of multilayer mirrors (MM). Such mirrors have already proved effective in various electromagnetic radiation ranges, however, the theoretical reflectivity limit of multilayer mirrors in the X-ray range is much lower than 100% due to strong radiation absorption by virtually all materials [1,2]. Notwithstanding that the authors in the previously published works [3–6] managed to achieve mirror reflection coefficients that were quite close to the theoretical limit, there are still wavelength ranges where much lower reflection coefficients are observed.

Progress in a number of research and development efforts is closely related to the development of existing MM synthesis technology. In particular, 17.1 nm X-ray solar astronomy requires an increase in the resolution of recording equipment and, therefore, the reflection coefficient of coatings must be increased [7,8]. Improvement of the existing multilayer optics and search for new compositions of multilayer mirrors to achieve high reflection coefficients in a lower short-wavelength band of 11–12 nm are important tasks for lithographic applications [5,6,9]. Due to a large number of mirrors in a lithography lens system, an increase in the MM reflection coefficient by only a few percent can significantly affect the cost benefits [10].

Due to physical features of interaction between X-ray radiation and a substance, search for more transparent materials for a soft X-ray spectrum is an important task, which inevitably involves a need for improvement of MM consisting of the chosen materials. The most valuable practical achievement in the multilayer X-ray optics is the ability to provide a high reflection coefficient in a relatively narrow wavelength range. This task is handled successfully

by $\{A/S\}_N$ type periodic binary X-ray mirrors, where A is the „absorber“, a strongly absorbing material, S is the „spacer“, a weakly absorbing material, N is the number binary layer periods. For various X-ray ranges, Be, B₄C, Si, Al, Sr, Y [3–7,11–13] are mainly used as a „spacer“ and Mo, Zr, Ru, Pd, Ag [3,5,6,11–13] are chosen as an „absorber“.

The authors of this work were the first to propose using Rb as a „spacer“ Rb, and using Ru and Al „absorbers“ together with it (while Al generally serves as a „spacer“). Ru/Rb and Al/Rb mirror configurations were improved to achieve the maximum reflectivity using the genetic algorithm [14,15].

1. Calculation of X-ray mirror reflectivity

For any X-ray optical elements, a complex form of the refractive index n is a typical quantity [1,2]:

$$n = n_0 + i \cdot k, \quad (1)$$

where k is responsible for radiation absorption, and the frequency dependence is expressed as

$$n = 1 - \frac{r_0}{2\pi} \lambda^2 \rho \mu (f_1 + i f_2), \quad (2)$$

where r_0 is the classical electron radius, λ is the wavelength (reciprocal of frequency), ρ is the material density; μ — is the molar mass of a material; f_1 and f_2 are atomic scattering factors [1]. Materials with the biggest difference in the real part of refractive index n_0 with the lowest absorption k are the most advantageous pair of materials for multilayer interference structure synthesis [16]. Materials chosen for the exploratory study of MM synthesis are shown in Figure 1. Dependences of the real and imaginary parts of

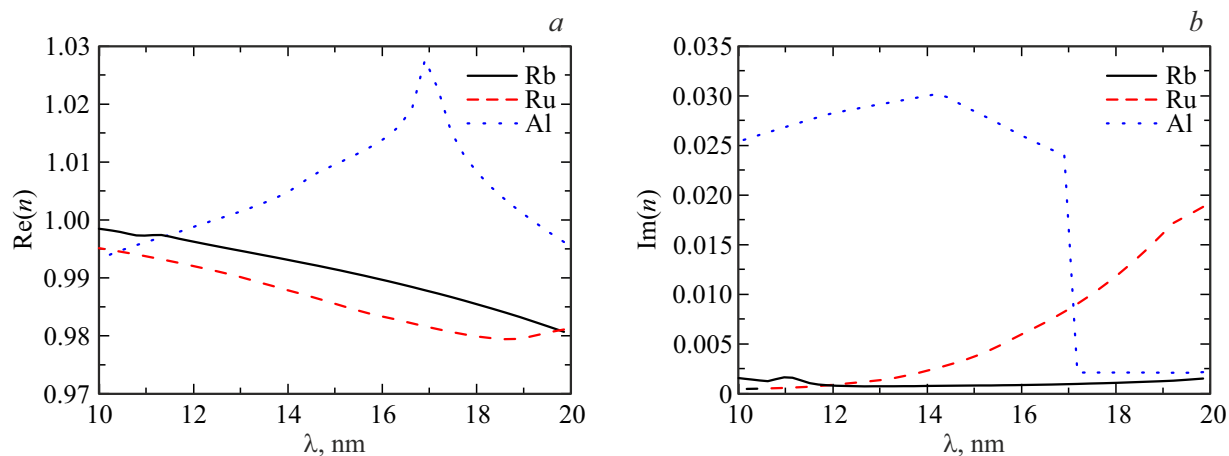


Figure 1. Real (*a*) and imaginary (*b*) parts of material refractive indices.

Table 1. Main properties of the improved Al/Rb mirror

Mirror configuration	Period d , nm	Number of periods N	Fraction of Al in a period $\beta_{\text{Al}} = h_{\text{Al}}/d$	Maximum reflection coefficient, %	Wavelength λ , nm	FWHM, nm
Al/Rb	8.5	125	0.41	83.3	17.04	0.20

refractive index on the radiation wavelength are also plotted in the figure.

The choice was conditioned by the fact that these elements had the biggest difference in the real parts of refractive index with the minimum imaginary parts in the wavelength range of interest ($\lambda = 11 - 17$ nm). However, it was noted that Rb showed the properties of the most transparent material (a material with the lowest absorption) in the soft X-ray region, thus providing the clear choice of the MM „spacer“ material.

The next step involved software implementation of the method for determining the multilayer structure reflectivity based on the solution to the Maxwell equations using a matrix method [17]. General theory of this calculation is described in [18–20]. Eventually, the authors received a tool for calculating MM reflection, transmission and absorption coefficients to provide an opportunity of further software suite upgrading. Due to the fact that the periodic mirror reflection maximum is related to the structure period (thickness of each of the layers) and to the angle of radiation incidence on MM, a solution to the improvement problem using a genetic algorithm was added to the software to satisfy the best mirror configuration selection criterion [14,15]. The target function was defined as the reflection coefficient function R depending on two variables (layer thicknesses h_1 and h_2), though there could be more control parameters (angle of radiation incidence, number of layers). But for reasons of time saving, it was proposed to examine these dependences separately of the improvement problem. Thus, the search for improvement was formed with preset initial conditions: mirror composition, number of layer pairs and

s-polarized radiation incidence direction. It was assumed that the mirror was ideal (free of roughness, layers were smooth and clearly defined) and the wavelength range of interest was $\lambda = 10 - 20$ nm. Improved calculations of the reflectivity of Al/Rb and Ru/Rb mirrors are shown below.

2. Al/Rb mirror

For MM, apart from the reflectivity dependence, radiation spectrum transmission FWHM, a spectral selectivity, was also of interest. The main properties of the improved Al/Rb mirror are shown in Table 1. Properties listed in the tables for all mirrors are hereinafter valid for normal radiation incidence.

Figure 2, *a* shows the dependence of the optimum Al/Rb mirror reflectivity on the wavelength, the mirror properties were taken from Table 1. Since the reflection coefficient curve also depends on the layer thickness ratio in a period, and the reflection maximum depends on the number of layers, then Figure 2, *b*, *c* shows the dependences of reflection on the fraction of strongly absorbing material (Al) in a period β_{Al} and the number of periods N , respectively. The curve in Figure 2, *b* also demonstrates the optimality of the proposed configuration parameters.

Figure 3 shows that the maximum MM reflection coefficient and the radiation bandwidth depend heavily on the angle of incidence, and at $\theta = 0 - 10^\circ$ the following may be achieved: 1) maximum reflection $R_{\text{max}} = 83\%$ with non-minimum FWHM = 0.2 nm; 2) minimum FWHM_{min} = 0.07 nm with mirror reflectivity $R = 58\%$. Therefore, note that parameterization of each

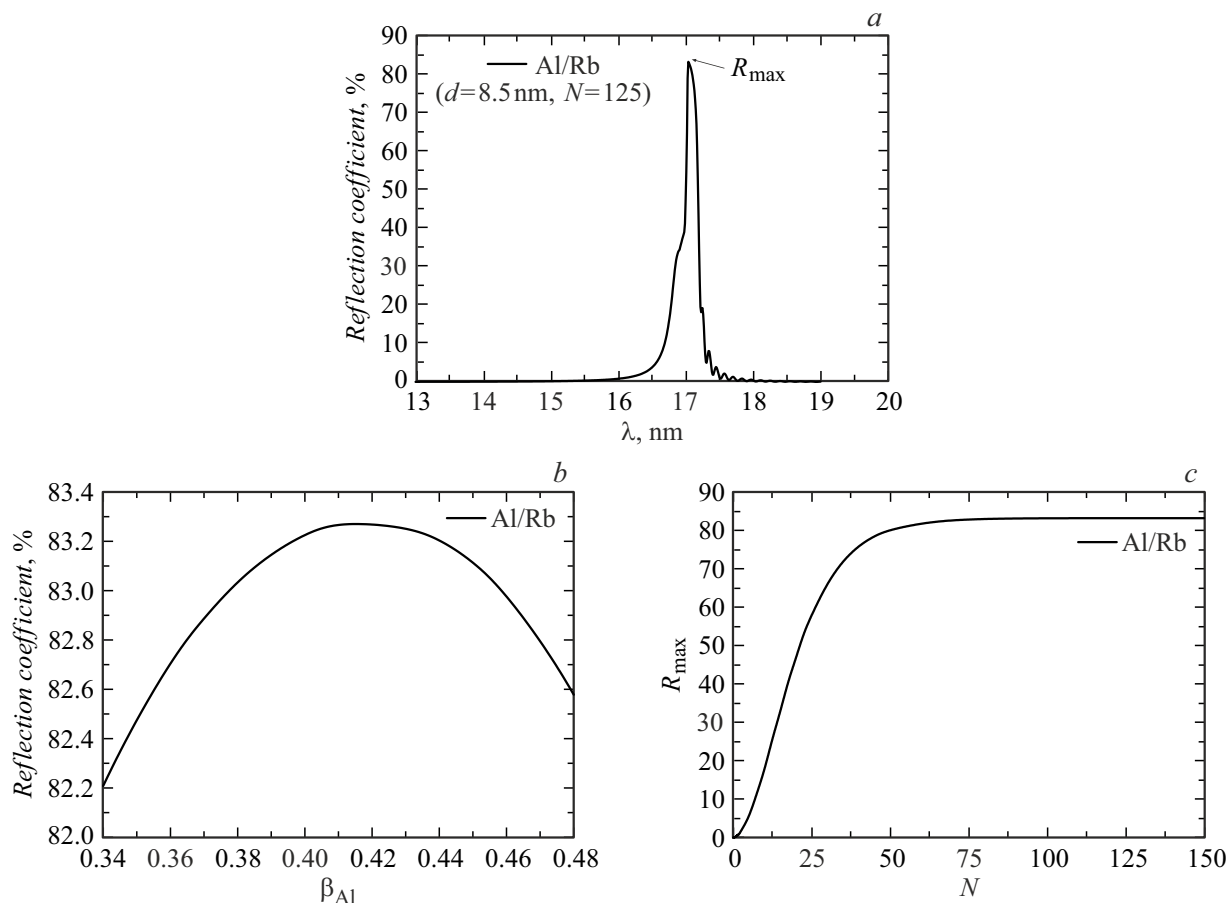


Figure 2. Dependences of Al/Rb mirror reflection coefficient on: *a* — incident radiation wavelength; *b* — fraction of Al in a period; *c* — number of MM periods.

MM depends on the particular future application of this mirror.

3. Ru/Rb mirror

Properties of the improved Ru/Rb mirror for $\lambda = 13.5$ nm are shown below (this wavelength corresponds to a modern lithography plasma source).

Figure 4–6 shows the dependences of mirror reflectivity on the wavelength, fraction of Ru in a period β_{Ru} , number of MM periods and angle of radiation incidence, and the dependences of the bandwidth on the angle of radiation incidence.

Review of Figure 5, *a* and 6, *b* shows that, by varying the angle of radiation incidence on the mirror, a higher MXM reflection may be achieved compared with the improved calculation. This is caused by the fact that the improvement was performed for a normal incidence mirror and only h_1 and h_2 were used as control parameters for the genetic algorithm. However, it is reasonable to assume that the increase in the Ru/Rb mirror reflectivity is related to approaching the Ru or Rb absorption edge (similar to approaching the *L*-absorption edge of Si in Mo/Si

mirrors [21]). Figure 7 visualizes the dependences of the real (n_0) and imaginary (k) parts of the complex refractive index $n = n_0 + i \cdot k$ for Ru and Rb on the wavelength calculated using the atomic scattering factors [1].

Figure 7, *d* shows that Rb has an absorption spike at $\lambda \sim 11 - 12$ nm in contrast to the smooth curve for Ru (Figure 7, *b*) suggesting that it is Rb that provides the increases in the Rb-based mirror reflectivities at the approach to the absorption edge.

Regardless of the fact that Ru/Rb mirrors were improved for $\lambda = 13.5$ nm, the mirror reflectivities obtained with varying angles of incidence are important results for $\lambda = 11 - 12$ nm because for the purpose of modern lithography they provide multilayer X-ray mirrors for a xenon-based or krypton-based plasma source with a theoretical reflection limit compared with that of Mo/Si mirrors that are currently successfully used with a $\lambda = 13.5$ nm source.

4. Discussion of findings

A special research interest of this work was in comparing the findings with current multilayer X-ray mirror solutions at: 1) $\lambda = 11 - 12$ nm for future next-generation lithog-

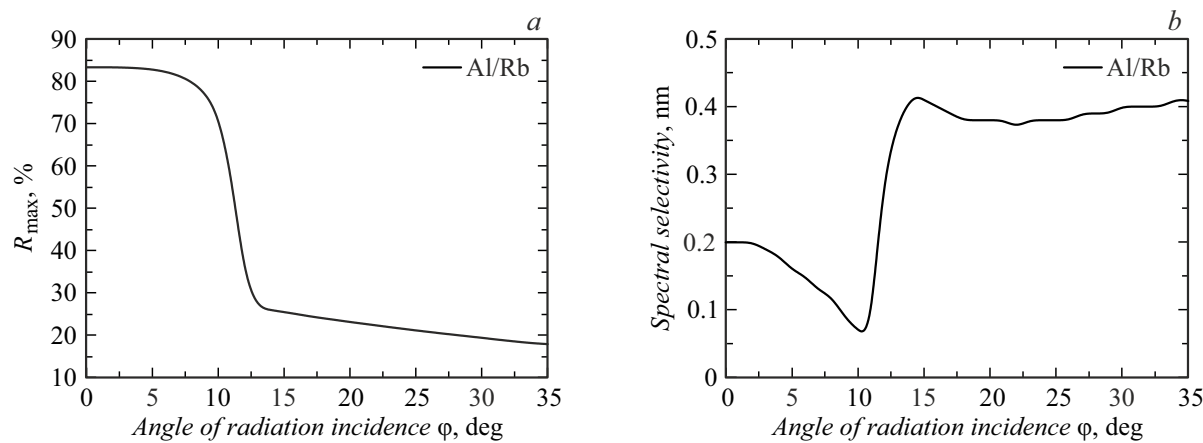


Figure 3. Dependence of the Al/Rb mirror parameters on the angle of radiation incidence on MM (0° corresponds to the normal incidence): *a* — maximum reflection; *b* — spectral selectivity FWHM.

Table 2. Main properties of the improved Ru/Rb mirror

Mirror configuration	Period d , nm	Number of periods N	Fraction of Ru in a period $\beta_{\text{Ru}} = h_{\text{Ru}}/d$	Maximum reflection coefficient, %	Wavelength λ , nm	FWHM, nm
Ru/Rb	6.8	125	0.23	77.9	13.5	0.54

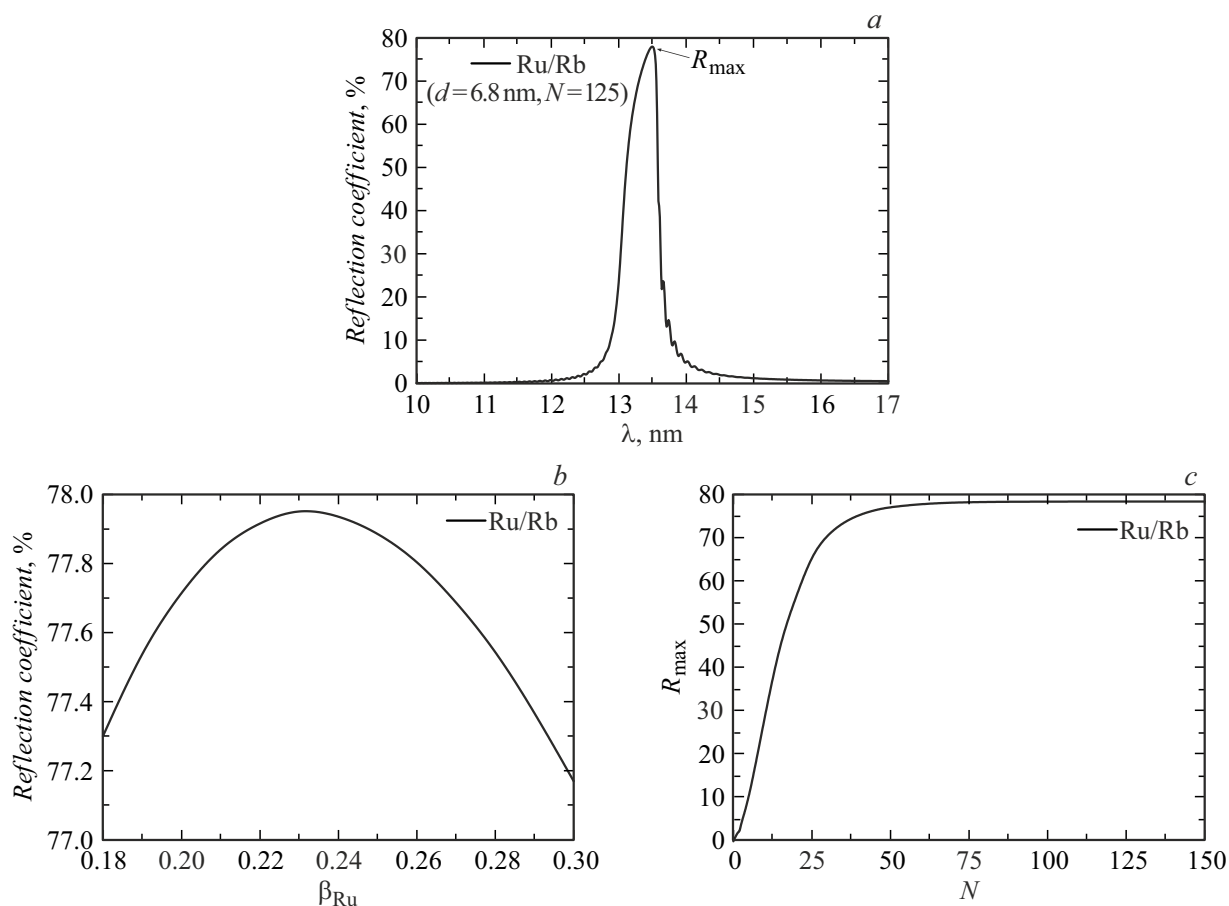


Figure 4. Dependences of Ru/Rb mirror reflection coefficient on: *a* — incident radiation wavelength; *b* — fraction of Ru in a period; *c* — number of MM periods.

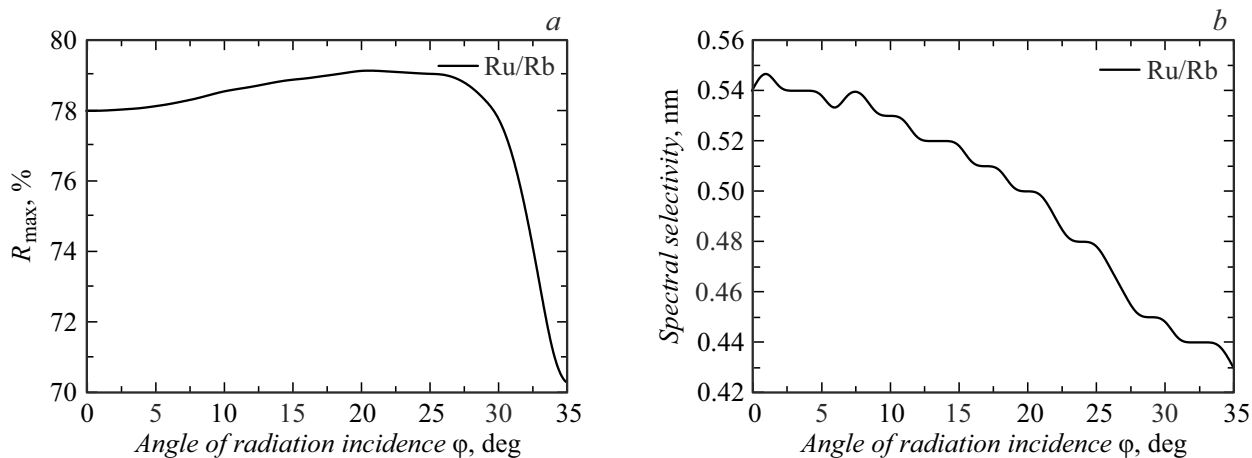


Figure 5. Dependence of the Ru/Rb mirror parameters on the angle of radiation incidence on MM (0° corresponds to the normal incidence): *a* — maximum reflection; *b* — spectral selectivity FWHM.

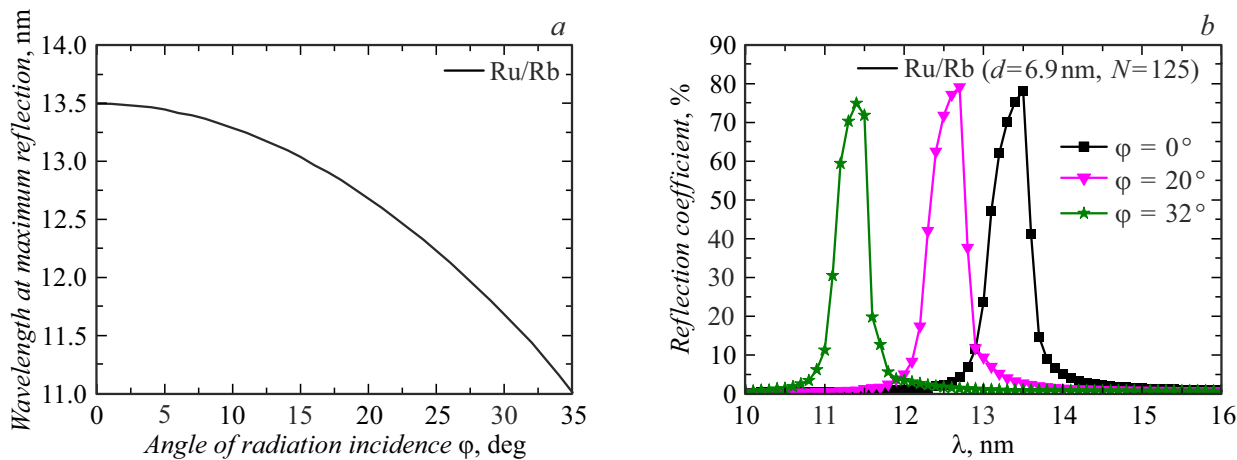


Figure 6. Dependence of the Ru/Rb mirror properties: *a* — correspondence of the wavelength at maximum reflection (λ at R_{\max}) (0° corresponds to the normal incidence); *b* — mirror reflectivity at various angles of radiation incidence.

raphy; 2) $\lambda = 13.5$ nm for modern lithography; 3) near $\lambda = 17.0 - 17.1$ nm for the X-ray astronomy. The Institute for Physics of Microstructures of the Russian Academy of Sciences (Institute for Physics of Microstructures of the Russian Academy of Sciences) studied yttrium-based MM for a spectral range of 8–12 nm [5] and Ru/Sr mirrors for 9–12 nm [6]. For lithography at $\lambda = 13.5$ nm, Mo/Si mirrors have already demonstrated their efficiency [3,22], however, a search is underway for solutions capable of increasing the reflectivity of such mirrors by decreasing the Mo and Si interdiffusion [3,23–25]. The foreign literature [23] proposed using Rb as an additive to Si due to its transparency in the lithography spectral range, which correlates with the findings of this work. For solar X-ray astronomy near $\lambda = 17$ nm, Be/Si/Al mirrors are considered to be the best [7,8]. Comparative analysis of the literature data and findings of this work is shown in Table 3.

Conclusion

The investigations of Rb-containing MM indicate that Rb-based structures provide high theoretical reflection coefficients with the lowest spectral selectivity for various X-ray ranges: for $\lambda = 11.4$ nm - the best result is provided by Ru/Rb mirrors with a reflection coefficient of 75% (FWHM ≈ 0.4 nm); for $\lambda = 13.5$ nm - the best result is provided by Ru/Rb mirrors with 78% (FWHM ≈ 0.5 nm); for $\lambda = 17.04$ nm - the best result is provided by Al/Rb mirrors with the highest possible reflection coefficient of $\sim 83\%$ (FWHM ≈ 0.2 nm). However, considering the high reactivity of Rb, feasibility of these mirrors in terms of practical implementation shall be evaluated. Notwithstanding that this problem is beyond the scope of this study, some theoretical assumptions may be provided. Pure Rb is known to be unstable in contact with air, but this doesn't make it impractical because, first, barrier layers may be used to separate Rb from the ambient air, and, second, the

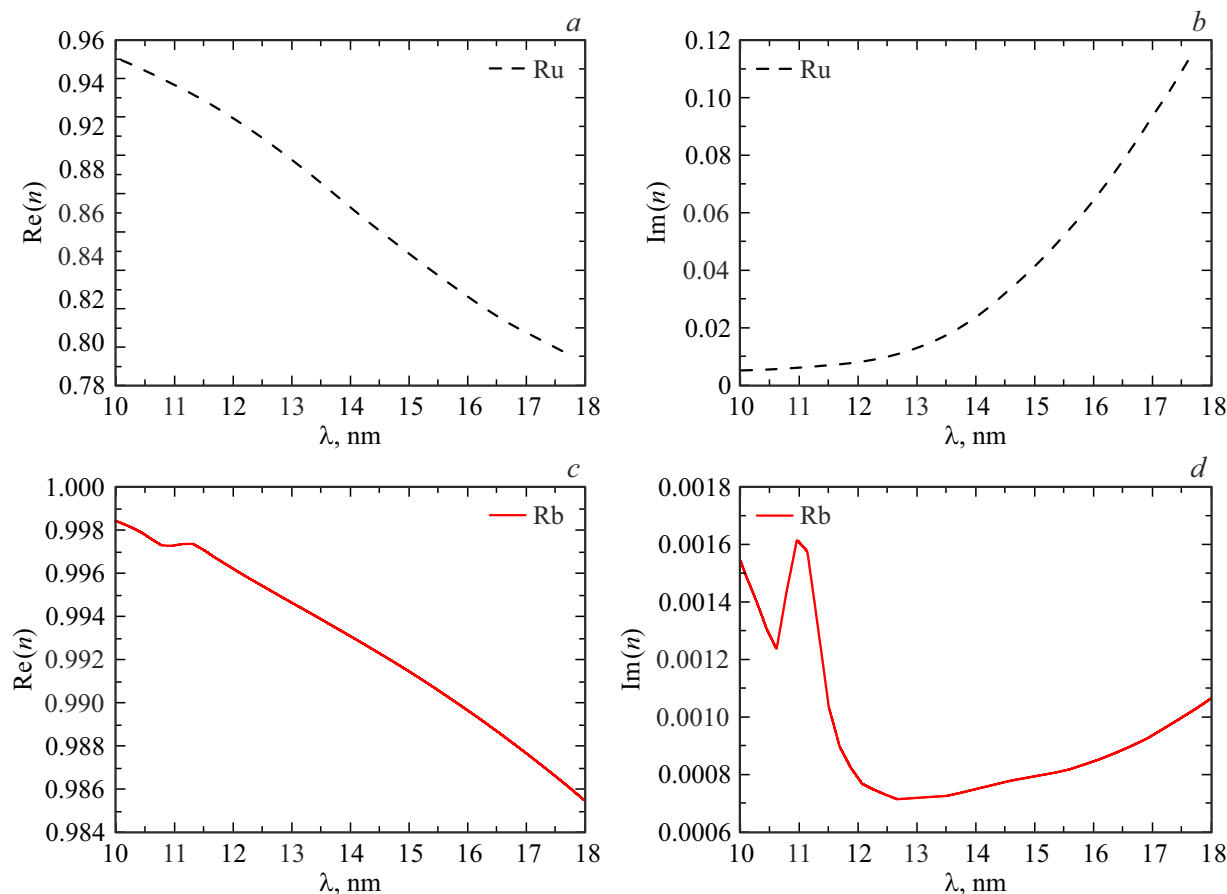


Figure 7. Dependences of the complex refractive index on the wavelength: *a* — real part of the refractive index of Ru; *b* — imaginary part of the refractive index of Ru; *c* — real part of the refractive index of Rb; *d* — imaginary part of the refractive index of Rb.

Table 3. Comparison of the literature data and the calculated MM data obtained in this work

Mirror configuration	Theoretical reflection limit, R_{\max}	Spectral selectivity FWHM, nm	Data source
Region $\lambda = 11.4$ nm			
Ru/Y	62 % (Practical result 56 %)	~ 0.35	[5]
Ru/Sr	~ 73 % (Practical result 62 %)	—	[6]
Ru/Rb	75 %	0.44	This work
Region $\lambda = 13.5$ nm			
Mo/Si	74 %	0.58	[3]
Mo/Be/Si	75 % (Practical result 72 %)	0.56	[3]
Mo/RbSi	75 %	—	[23]
Ru/Rb	78 %	0.54	This work
Region $\lambda = 17.0 - 17.1$ nm			
Be/Si/Al	75 % (Practical result 61 %)	0.40	[7,8]
Al/Rb	83 %	0.20	This work

multilayer structure is form in such a way that the edge layer in contact with air is Ru, an inert material that can serve as a protective coating on its own. In addition, multilayer mirrors are manufactured and used in vacuum conditions, therefore all proposed Rb-containing mirrors may be suitable for lithography purposes provided that the proper preparation and treatment procedures are fulfilled [23].

Since the theoretical research results demonstrate the practical value of Rb-based multilayer structures for applications in the spectral range of 11–17 nm, the authors are planning to continue their work in the form of experimental support of calculations and a search for not less transparent, but at the same time chemically stable Rb-containing compounds and alloys.

Conflict of interest

The authors declare no conflict of interest.

References

- [1] B.L. Henke, E.M. Gullikson, J.C. Davis. *Atomic Data and Nuclear Data Tables*, **54** (2), 181 (1993).
- [2] A. Michette. *Optika myagkogo rentgenovskogo izlucheniya* (Mir, M., 1989) (in Russian)
- [3] N. Chkhalo, S. Gusev, A. Nechay, D. Pariev, V. Polkovnikov, N. Salashchenko, F. Schäfers, M. Sertsu, A. Sokolov, M. Svechnikov, D. Tatarsky. *Opt. Lett.*, **42** (24), 5070 (2017). DOI: <https://doi.org/10.1364/OL.42.005070>
- [4] Yu.A. Weiner, S.A. Garakhin, S.Yu. Zuev, A.N. Nechai, R.S. Pleshkov, V.N. Polkovnikov, N.N. Salashchenko, M.V. Svechnikov, M.G. Sertsu, R.M. Smertin, A. Sokolov, N.I. Chkhalo, F. Shafers. *Poverkhnost'. Rentgenovskie, sinhrotronnye i neutronnye issledovaniya* **2**, 3 (2020) (in Russian). DOI: 10.31857/S1028096020020168
- [5] V.N. Polkovnikov, R.A. Shaposhnikov, N.I. Chkhalo, N.N. Salashchenko, N.A. Dyuzhev, F.A. Pudonin, G.D. Demin. *Kratkie soobshcheniya po fizike FIAN*, **12**, 58 (2021) (in Russian).
- [6] R.A. Shaposhnikov, S.Yu. Zuev, V.N. Polkovnikov, N.N. Salashchenko, N.I. Chkhalo. *ZhTF*, **92** (8), 1179 (2022) (in Russian). DOI: 10.21883/JTF.2022.08.52780.124-22
- [7] S.V. Kuzin, A.A. Reva, S.A. Bogachev, N.F. Erkhova, N.N. Salashchenko, N.I. Chkhalo, V.N. Polkovnikov. *ZhTF*, **90** (11), 1817 (2020) (in Russian). DOI: 10.21883/JTF.2020.11.49967.113-20
- [8] N.I. Chkhalo, D.E. Pariev, V.N. Polkovnikov, N.N. Salashchenko, R.A. Shaposhnikov, I.L. Stroulea, M.V. Svechnikov, Yu.A. Vainer, S.Yu. Zuev. *Thin Solid Films*, **631**, 106 (2017). DOI: 10.1016/j.tsf.2017.04.020
- [9] A.D. Akhsakhalyan, E.B. Klyuenkov, A.Ya. Lopatin, V.I. Luchin, A.N. Nechai, A.E. Pestov, V.N. Polkovnikov, N.N. Salashchenko, M.V. Svechnikov, M.N. Toropov, N.N. Tsybin, N.I. Chkhalo, A.V. Shcherbakov. *Poverkhnost'. Rentgenovskie, sinhrotronnye i neutronnye issledovaniya* **1**, 5 (2017) (in Russian).
- [10] V.N. Polkovnikov, N.N. Salashchenko, M.V. Svechnikov, N.I. Chkhalo. *YFN, ser. „Konferentsii i simpoziumy“*, **190** (1), 92 (2020) (in Russian). DOI: <https://doi.org/10.3367/UFNr.2019.05.038623>
- [11] E.A. Vishnyakov, D.L. Voronov, E.M. Gullikson, V.V. Kondratenko, I.A. Kopylets, M.S. Luginin, A.S. Pirozhkov, E.N. Ragozin, A.N. Shatokhin. *Kvant. elektron.*, **43** (7), 666 (2013) (in Russian).
- [12] R.A. Shaposhnikov, S.Yu. Zuev, V.N. Polkovnikov, N.N. Salashchenko, N.I. Chkhalo, F. Delmotte, E. Melchakov. *ZhTF*, **89** (11), 1774 (2019) (in Russian). DOI: 10.21883/JTF.2019.11.48343.129-19
- [13] E.A. Vishnyakov, F.F. Kamenets, V.V. Kondratenko, M.S. Luginin, A.V. Panchenko, Yu.P. Pershin, A.S. Pirozhkov, E.N. Ragozin. *Kvant. elektron.* (in Russian), **42** (2), 143 (2012).
- [14] T.V. Panchenko. *Geneticheskie algoritmy: uchebno-metodicheskoe posobie* (Izdat. dom „Astrakhansky universitet“, Astrakhan, 2007) (in Russian)
- [15] M.M. Barysheva, S.A. Garakhin, S.Yu. Zuev, V.N. Polkovnikov, N.N. Salashchenko, M.V. Svechnikov, R.M. Smertin, N.I. Chkhalo, E. Melchakov. *ZhTF*, **89** (11), 1763 (2019). DOI: 10.21883/JTF.2022.08.52770.118-22
- [16] S.A. Garakhin, A.Ya. Lopatin, A.N. Nechay, A.A. Perekalov, A.E. Pestov, N.N. Salashchenko, N.N. Tsybin, N.I. Chkhalo. *ZhTF*, **93** (7), 1002 (2023) (in Russian). DOI: 10.21883/JTF.2023.07.55760.60-23
- [17] Yu.A. Novikova. *Avtoref. kand. diss.* (Gos. un-t aerokosmicheskogo proborostroeniya, SPb, 2015) (in Russian)
- [18] F. Abeles. *Ann. Phys.*, **3** (4), 504 (1948).
- [19] Born, E. Volf, *Osnovy optiki* (Nauka, M., 1970), p. 720 (in Russian).
- [20] P.H. Berning. *Teoriya i metody rascheta opticheskikh svoistv tonkikh. Sb. fizika tonkikh plenok* (Mir, M., 1967) [Pod. obshch. red. G. Hassa n R.E. Tauna; perevod c angl. pod. red. V.B. Sandomirskogo A.G. Zhdana] (in Russian)
- [21] N. Kaiser, S. Yulin, M. Perske, T. Feigl. *Proceedings in SPIE*, **7101**, 71010Z-1 (2008). DOI: 10.1117/12.796150
- [22] S. Bajt, J.B. Alameda, T. Barbee, W.M. Clift. *Proceedings in SPIE, Optical Engineering*, **41** (8), 1797 (2002). DOI: 10.1117/1.1489426
- [23] M. Saedi, C. Sfiligoj, J. Verhoeven, J.W.M. Frenkena. *Appl. Surf. Sci.*, **507**, 1 (2020). DOI: <https://doi.org/10.1016/j.apsusc.2019.144951>
- [24] E. Louis, A.E. Yakshin, P.C. Görts, S. Oestreich, R. Stuik, M.J.H. Kessels, E.L.G. Maas, F. Bijkerk, M. Haidl, S. Muel-lender, M. Mertin, D. Schmitz, F. Scholze, G. Ulm. *Proc. SPIE*, 3997, (2000). DOI: 10.1117/12.390077
- [25] S.A. Yulin, I.V. Kozevnikov, S.I. Sagitov, V.A. Chirkov, V.E. Levashov, A.V. Vinogradov. *Appl. Opt.*, **32** (10), 1811 (1993).

Translated by E.Ilinskaya